X-ray spectromicroscopy study of competitive adsorption of protein and peptide onto polystyrene-poly(methyl methacrylate)

Bonnie O. Leung and Adam P. Hitchcock[a)]
BIMR, TuesduesMcMaster University, Hamilton, Ontario, Canada L8S 4M1

John L. Brash
School of Biomedical Engineering, McMaster University, Hamilton, Ontario, Canada L8S 4L8

Andreas Scholl and Andrew Doran
Advanced Light Source, Lawrence Berkeley National Laboratory, Berkeley, California 94720

Peter Henklein
Institut fur Biochemie, Universitatsklinikum Charite, Humboldt-Universitat, 10117 Berlin, Germany

Joerg Overhage, Kai Hilpert, John D. Hale, and Robert E. W. Hancock
Department of Microbiology and Immunology, University of British Columbia, Vancouver, British Columbia, Canada V6T 1Z4

(Received 29 April 2008; accepted 19 June 2008; published 24 July 2008)

A synchrotron-based x-ray photoemission electron microscope (X-PEEM) was used to investigate the coadsorption of a mixture of human albumin serum and SUB-6, a synthetic antimicrobial peptide, to a phase-segregated polystyrene/poly(methyl methacrylate) (PMMA) substrate at varying concentrations and *p*H. The authors show that X-PEEM could detect the peptide adsorbed from solution at concentrations as low as $5.5\times10^{-9}M$ and could differentiate the four components via near-edge x-ray absorption fine structure spectromicroscopy. At neutral *p*H the SUB-6 peptide adsorbed preferentially to PMMA. At a *p*H of 11.8 where the charge on the peptide was neutralized, there was a more balanced adsorption of both species on the PMMA domains. The authors interpret these observations as indicative of the formation of an electrostatic complex between positive peptide and negative protein at *p*H of 7.0. This solution complex had an adsorption behavior that depended on the polarity of the substrate domains, and favored adsorption to the electronegative PMMA regions. At a *p*H of 11.8 the complex formation was suppressed and a more competitive adsorption process was observed. © *2008 American Vacuum Society.* [DOI: 10.1116/1.2956637]

I. INTRODUCTION

Synchrotron-based soft x-ray microscopy[1–3] using near-edge x-ray absorption fine structure (NEXAFS) contrast is a useful tool for acquiring information on soft matter, in particular, polymeric and biological materials. In fact, NEXAFS spectromicroscopy is well suited for visualizing macromolecular subcomponents by differentiating between polysaccharides, nucleic acids, lipids, and proteins without the use of external probes.[4] NEXAFS is also an excellent tool to differentiate among amino acids and small peptides.[5–7] However, distinguishing one type of protein from a multitude of types of proteins[8] is difficult due to the fundamental similarity of the NEXAFS spectra of all proteins, which arises from the strong local sensitivity of the spectroscopy combined with spectral averaging over relatively similar distributions of amino acids. Nonetheless, since each amino acid yields a unique NEXAFS spectrum,[5,6] proteins or peptides containing an unusual sequence may be identified in favorable cases.[7,8]

Recently, a program was developed to predict the experimental carbon, nitrogen, and oxygen 1*s* NEXAFS spectra of any protein or peptide by means of spectral summation over its amino acid sequence.[7] Using this approach, the arginine-rich synthetic antimicrobial cationic peptide SUB-6 ($RWWKIWVIRWWR\text{-}NH_2$) (Ref. 9) was identified as a suitable candidate for mapping against the blood protein human serum albumin (HSA), via a characteristic transition at 289.3 eV from the guanidine group of arginine. Subsequent scanning transmission x-ray microscopy (STXM) experiments of SUB-6 dusted on a background of HSA easily identified and distinguished between the two biocomponents.[7] Charged antimicrobial peptides are of particular interest due to their ability to disrupt cytoplasmic membranes in bacterial cells. Thus, locating and mapping these peptides among other peptides and proteins within cells can aid in understanding the mechanisms of antimicrobial action and resistance.

We are interested in using soft x-ray spectromicroscopy techniques to visualize proteins or peptides in complex matrices that model environments such as biofilms or initial interactions of biological components with existing candidate biomaterials. Previous studies of blood protein adsorption to polymeric phase-segregated polystyrene (PS)—poly(methyl methacrylate) (PMMA) thin films demonstrated that surface sensitive x-ray photoemission electron microscopy (X-PEEM)[10–13] is complementary to STXM, with the capability of probing submonolayer protein-surface interactions. Systematic studies of the concentration dependence,[11]

[a)]Author to whom correspondence should be addressed; electronic mail: aph@mcmaster.ca

exposure time,[11] and effect of *p*H (Ref. 12) on HSA adsorption to PS/PMMA films suggest that protein adsorption is strongly influenced by hydrophobic effects. Moreover, a recent X-PEEM study of competitive adsorption of HSA and the blood-clotting protein fibrinogen (Fg) to PS/PMMA found that the NEXAFS spectra of HSA and Fg are too similar to be distinguished.[13]

The aim of this work was to investigate whether X-PEEM can be used to differentiate SUB-6 and HSA in a mixed adsorption on a phase-segregated polymer surface and, if so, to examine the competitive adsorption of protein and peptide. Previously, we had identified the hydrophobic effect as being important in determining adsorption sites of proteins (Fg and HSA) on the PS/PMMA substrate.[10–13] At neutral *p*H HSA in its native form has a substantial negative charge (~ -15) while SUB-6 is highly positive (+5). By changing the *p*H, the charge on these two species can be changed thus providing a direct probe of potential electrostatic interactions which might be expected to occur between the protein and peptide in solution, and thus might play a role in adsorption to polymer surfaces. The present results, combined with other studies of competitive protein adsorption,[13] are part of a larger program to evaluate the strengths and weaknesses of soft x-ray spectromicroscopy for mapping similar biocomponents on a complicated background matrix.

II. EXPERIMENT

A. Materials

Polystyrene [molecular weight (MW) of 1.07×10^{-6}, δ 1.06] and poly(methyl methacrylate) (MW of 312 000, δ 1.01) were purchased from Polymer Source Inc. and used as received. Thin films were prepared by dissolving PS and PMMA 30:70 (wt%/wt%) in toluene and then spun cast onto clean native oxide silicon wafers [Si(111)] at 4000 rpm for 40 s. Before spin coating, the Si wafers were vigorously degreased with 10 min sonication with trichloroethylene, acetone, and methanol followed by extensive rinsing with doubly distilled de-ionized water. The PS/PMMA substrates were annealed below 160 °C for 12 h in a vacuum oven at a pressure $\sim10^{-5}$ Torr, achieved with a cryotrapped turbo pump. Noncontact mode atomic force microscopy was used to verify the topology of the thin films and revealed discrete PMMA domains approximately 500–1000 nm wide within a continuous PS phase. The total film thickness was $\sim$40 nm with a measured corrugation of 4–8 nm. As observed previously, both the PS and PMMA domains contain microdomains of the opposite phase that are approximately 50–200 nm wide.[14]

Human serum albumin (HSA) was obtained from Behringwerke AG, Marburg, Germany, and found to be homogeneous as judged by sodium dodecyl sulfate polyacrylamide gel electrophoresis (SDS-PAGE). The SUB-6 peptide ($RWWKIWVIRWWR\text{-}NH_2$) was prepared by Henklein with 9-fluorenylmethyl carbamate solid-phase synthesis and purified by high-performance liquid chromatography and mass spectrometry.[15]

B. Protein/peptide exposure

The PS/PMMA substrate (8×8 mm^2) was placed in a 50 ml beaker, covered with 5 ml of peptide or protein/peptide mixture solution (varied concentrations) for 20 min and then diluted three times with at least 50 ml of doubly de-ionized (DDI) water. The substrate was removed and then vigorously rinsed with DDI water. The protein/peptide adsorbed sample was then carefully dried by touching the edge of the Si wafer with lens paper.

C. X-PEEM

The X-PEEM data were collected at the Advanced Light Source (ALS) on the PEEM-2 microscope at bending magnet beamline 7.3.1. Detailed accounts of the experimental apparatus, beamline setup, and instrument optics have been presented previously.[16] In brief, photoelectrons and secondary electrons ejected by absorption of 70%–80% right circularly polarized [a mask in the beamline is used to select below plane (right circularly polarized) radiation], monochromatic x rays are accelerated into an electrostatic imaging column, where the spatial distribution is magnified and detected by a charge coupled device (CCD) camera. X-PEEM is a surface sensitive technique with a sampling depth ($1/e$) of 4 nm for polymers,[17] with integrated signals sampling the top 10 nm of the sample. Image sequences (stacks[18]) were recorded at the C 1*s* and N 1*s* edge. A 100-nm-thick Ti filter was used to eliminate second-order light. To minimize radiation damage, a fast shutter (0.1*s*) was used to block the beam except during data acquisition. This reduced the x-ray exposure by 50% by blocking the beam during the time required to transfer images from the CCD camera and to step the photon energy. The incident flux was reduced to about 10% of the full intensity by masking upstream of the monochromator, and a limited number of energies (23 in C 1*s*, 46 in N 1*s*) and a short exposure time (1*s*) per image were used as other ways to minimize radiation damage. The field of view was approximately 20 μm.

D. STXM

All STXM data were collected at beamline 5.3.2 at the ALS.[19,20] Typically, solvent-cast samples with thickness below 100 nm were analyzed by collecting micrometer sized stacks. Image sequences[18] were used in homogeneous areas to minimize radiation damage. An image at a damage sensitive energy was recorded after each spectral measurement to ensure negligible damage.

III. DATA ANALYSIS

A. Reference spectra

High quality NEXAFS reference spectra of PS, PMMA, HSA, and SUB-6 peptide[7] were obtained with STXM on films floated onto (PS/PMMA) or solvent cast upon (HSA, SUB-6) a silicon nitride window. Furthermore, the linear absorbance was set to an absolute scale by normalizing outside the edge region to the elemental response of 1 nm at bulk

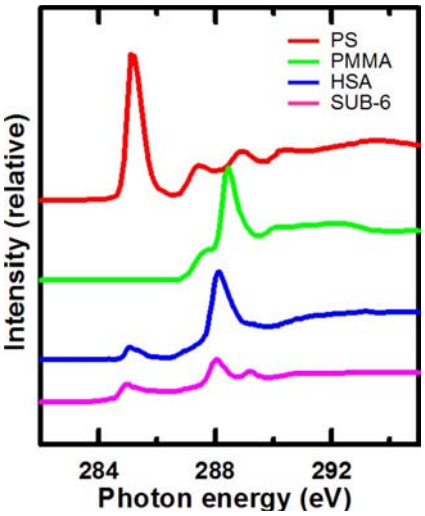

FIG. 1. C 1*s* x-ray absorption spectra of polystyrene (PS, red), poly(methyl methacrylate) (PMMA, green), human serum albumin (HSA, blue), and the peptide, SUB-6 (pink) recorded from pure materials. The spectra are plotted on an absolute linear absorbance scale.

densities computed from tables of elemental x-ray absorption.[21] Although NEXAFS spectra obtained with STXM are collected in transmission rather than total electron yield mode, the spectra from both detection schemes exhibit the same shapes. The STXM reference spectra were used since they are better resolved (energy resolution of 0.1–0.2 eV) compared to X-PEEM (energy resolution of 0.4–0.5 eV).

The reference spectra for PS, PMMA, HSA, and SUB-6 are shown in Fig. 1. The spectrum of each species has characteristic features which allow differentiation from each of the other components. PS is characterized by a C 1*s* $\rightarrow \pi^*_{C=C}$ transition at 285.15(3) eV. PMMA and HSA exhibit strong C 1*s* $\rightarrow \pi^*_{C=O}$ transitions at 288.45(3) and 288.20(3) eV, respectively. The shift to lower energy for the protein relative to PMMA arises from the less electronegative environment of the carbonyl carbon in R-CONH peptide bonds compared to that in the R-COOMe ester functional group of PMMA. The C 1*s* spectrum of SUB-6 is readily identified from its strong C 1*s* $\rightarrow \pi^*$(C=N) transition at 289.37(3) eV, as well as significant intensity in the 286–287 eV region from C 1*s*(C−R) $\rightarrow \pi^*_{C=C}$ transitions.

B. Chemical mapping and quantitative analysis

Each image sequence was aligned if needed, normalized to the ring current, and divided by the I_o signal. The I_o spectrum is that measured from a piece of HF-etched Si(111), corrected by the adsorption spectrum of Si and a linear energy term which accounts for the bolometric response of PEEM detection. The energy scale was calibrated by assigning the peak of the C 1*s* $\rightarrow \pi^*_{C=C}$ transition of PS to 285.15 eV. All data manipulations were performed using aXis2000.[22]

The spectrum at each pixel of the image sequence was fit to linear combinations of reference spectra using singular value decomposition, which is an optimized method of performing least-squares fits in the cases of highly overdetermined data sets.[23,24] The resulting fit coefficients are collected into component maps which display the spatial distribution of each chemical component. Illumination correction was applied by dividing by a heavily smoothed version of the sum of all component maps. Typically, the illumination varied by less than 10% over the area studied. The intensity scale of each component map was set to an absolute thickness value by dividing by a scale factor determined by setting the average total thickness (determined by adding all component maps) to 10 nm.[17] The total thickness maps typically had residual fluctuations of 15%–20% which were largest in the PMMA domains (see Fig. 2 of Ref. 12).

Pixels of areas specific to PS or PMMA were selected by applying a threshold mask to the PS and PMMA component maps—i.e., only pixels having a signal above a defined value are included. The interface was specified as areas not present in either the PS or PMMA masked areas. The spectrum extracted from each region (PS, PMMA, and interface) was further modified by setting the pre-edge region to zero intensity followed by adjustment of the absorption scale to obtain a total thickness of 10 nm. The background subtracted and normalized spectrum extracted from each region was then fit using the same reference spectra as used to derive the component maps. Several stacks were obtained from each sample and the compositional results from these independent repeat measurements were averaged to yield the final quantitative results. The uncertainties cited in the tables are the standard deviations from these multiple determinations.

IV. RESULTS AND DISCUSSION

A. X-PEEM detection limits

The NEXAFS spectrum of SUB-6 is primarily distinguished from those of PS, PMMA, and HSA by the C 1*s* $\rightarrow \pi^*_{C=N}$ transition at 289.37 eV and also via a small C 1*s*(C−R) $\rightarrow \pi^*_{ring}$ contribution at 286.0 eV,[8] shown in Fig. 1. Careful analysis of the curve-fitting results revealed that the dip at 286.0 eV in the fit reported by the least-squares refinement was too large, leading to an overestimation of the peptide thickness value. Thus, baseline control fitting procedures were performed to verify the minimum detectable amount of SUB-6. Figure 2 plots spectra of the PS, PMMA, and interface regions of a pure PS/PMMA substrate along with the result of optimized curve fits to the PS, PMMA, and SUB-6 reference spectra. Table I summarizes the quantitative results. The spectrum obtained from the PS region was dominated by the aromatic transition at 285.15 eV and the small contribution from PMMA yielded a less intense transition at 288.50 eV that masked the SUB-6 contribution from the transitions at both 288.50 and 289.37 eV. In contrast, the higher $\pi^*_{C=O}$ intensity for the PMMA and interface regions allowed for more flexible fits of SUB-6 in the region 287.5–289.5 eV leading to peptide thickness values close to 1.5(5) nm.

Energy calibration plays a key role in accurate determination of the protein and peptide components. If the energy

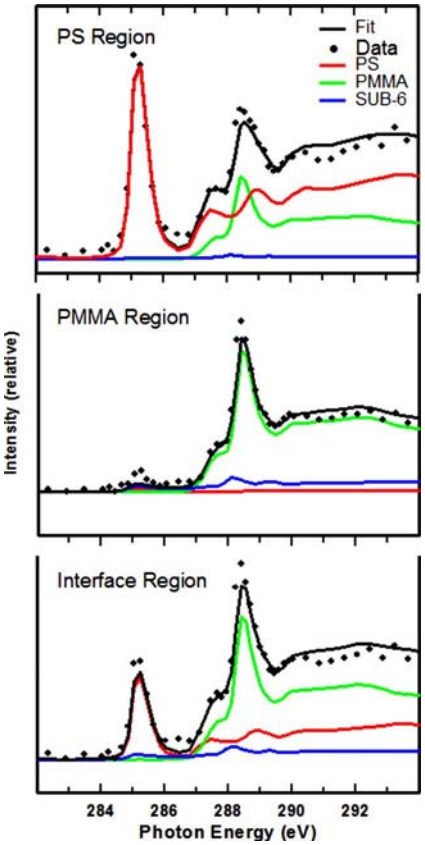

FIG. 2. Curve fits to the average C 1*s* spectra extracted from the PS, PMMA, and interface regions of a pure PS/PMMA blend (no adsorbed protein or peptide). Image sequence recorded using the ALS polymer STXM.

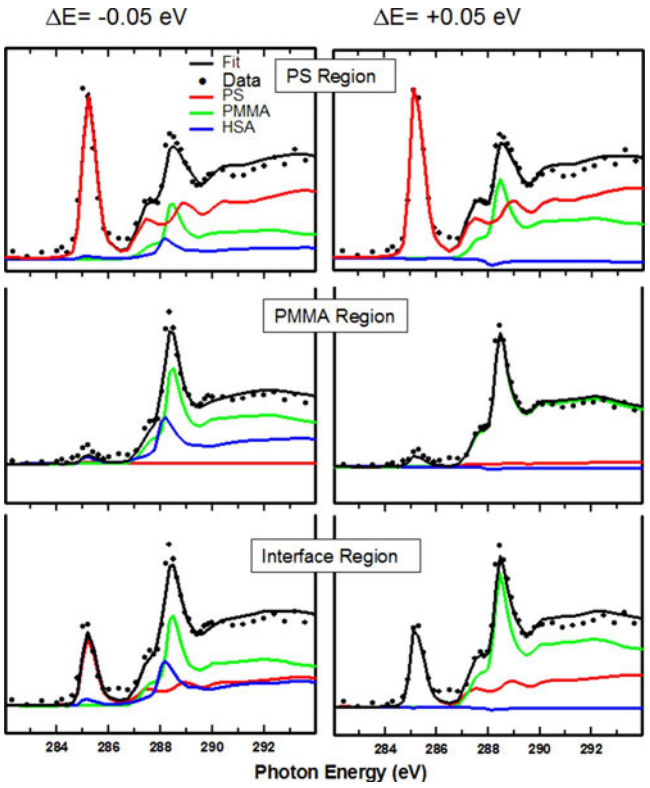

FIG. 3. Left column is the result of curve fits to the PS/PMMA spectra with the energy scale shifted 0.05 eV lower than the correct values, while the right column is the result for an energy scale shifted +0.05 eV. The amounts of HSA and SUB-6 derived from this analysis represent a worst case result from energy miscalibration causing a misassignment of adsorbed protein or peptide, and thus correspond to a conservative evaluation of the detection limits.

scale is miscalibrated to a lower energy by even 0.05 eV, then the amount of protein is overestimated. If it is miscalibrated to a higher energy by a similar amount, the amount of PMMA is overestimated. Details of this potential systematic error are presented in Fig. 3. Nonetheless, if appropriate measures are taken it is possible to reliably calibrate the energy scale using the 285.15 eV PS peak to better than 0.02 eV. Based on these studies the minimum detectable amount of HSA was conservatively estimated to be 1.0(5) nm (Table I).

TABLE I. Analysis of *C* 1*s* spectra of a clean PS/PMMA substrate with inclusion of SUB-6 and HSA components to evaluate the minimum detectable amount of protein/peptide. Uncertainty is ±0.5 nm.

		Thickness of SUB-6 or HSA on PS/PMMA (nm)	
Region	Composite (nm/pixel)	SUB-6	HSA
PS	PS	8.8	8.8
	PMMA	1.0	0.4
	HSA	⋯	0.7
	SUB-6	0.2	…
PMMA	PS	2.8	3.1
	PMMA	5.7	5.8
	HSA	⋯	1.1
	SUB-6	1.5	⋯
Interface	PS	5.5	5.9
	PMMA	3.2	2.8
	HSA	⋯	1.3
	SUB-6	1.3	⋯

B. Concentration dependence of the specific adsorption of SUB-6

The adsorption of SUB-6 on the PS/PMMA surface was probed as a function of concentration to determine the specific adsorption of the cationic peptide. Three concentrations were investigated: 1×10^{-2}, 1×10^{-4}, and 1×10^{-5} mg/ml in de-ionized water, in each case using a fixed adsorption time of 20 min. Color-coded composite maps are presented in Fig. 4 with two different presentations of the same data. The maps on the right were rescaled such that the intensity of each component was mapped separately to the full range of its color (0–255), thereby highlighting the spatial distribution of the peptide relative to the polymer substrate. The limits of the R (PS), G(PMMA), B(SUB-6) color bars indicated the range for each component. The maps on the right are displayed on a common thickness scale (0–10 nm), which preserved the absolute thickness information.

The rescaled maps indicate that the peptide selectively adsorbed to the interface between PS and PMMA, which was

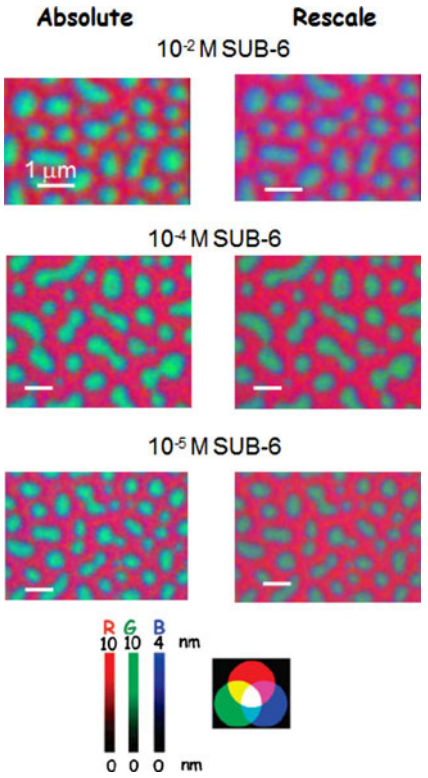

FIG. 4. Color-coded component maps (left, absolute; right, rescaled) for a PS/PMMA blend exposed for 20 min to three different concentrations of SUB-6—(top) 1×10^{-2} mg/ml, (middle) 1×10^{-4} mg/ml, and (bottom) 1×10^{-5} mg/ml.

previously shown to be the preferred site of adsorption, and thus the area of the lowest free energy.[10] The three maps were virtually identical with the exception of the width of adsorbed protein at the interface which became successively wider as the concentration increased. The absolute maps demonstrate that more peptide was adsorbed at higher concentration on the PMMA domains, which are significantly bluer than the domains at lower concentration.

These results were verified by the quantitative analysis of spectra extracted from the images by threshold masking (Table II). Over the three concentrations sampled, the peptide exhibited preferential adsorption to both the interface and PMMA regions over the PS region, which remained strikingly bare. These trends were reversed in comparison to the adsorption of the negatively charged HSA, which showed greater preference for the nonpolar PS compared to polar PMMA.[11] Since SUB-6 has a positive (+5) charge (if all amino groups are protonated), it should be significantly more attracted to the electronegative ester groups of PMMA, thus explaining the pronounced selectivity for SUB-6 adsorption on the PMMA domains.

SUB-6 showed the strongest preference for both the interface and the PMMA regions. As the concentration was lowered, the adsorption decreased across all regions, especially on the PS domains. This is not surprising since the free energy of the system would be decreased more by adsorption on the interdomain interfaces than on the domains themselves, and the highly positive SUB-6 would be strongly attracted to the polar carbonyl groups of PMMA.

TABLE II. Thickness of SUB-6 (nm/pixel) on the PS and PMMA domains and at the PS/PMMA interface for adsorption of SUB-6 on a PS/PMMA blend at three concentrations. Uncertainty is ±0.5 nm.

		Thickness (nm) SUB-6 concentration (mg/ml)		
Region	Composite (nm/pixel)	1×10^{-2}	1×10^{-4}	1×10^{-5}
PS	PS	8.4	9.7	9.2
	PMMA	0.5	0.2	0.8
	SUB-6	1.1	0.1	0.0
PMMA	PS	2.2	2.5	4.4
	PMMA	4.8	6.0	4.3
	SUB-6	3.0	1.4	1.3
Interface	PS	3.6	5.6	6.7
	PMMA	2.1	3.2	2.1
	SUB-6	4.2	1.3	1.1

C. HSA and SUB-6 competitive adsorption

Figures 5 and 6 show the rescaled and absolute color-coded component maps of HSA and SUB-6 adsorption on PS/PMMA. In each map PS is coded in red, PMMA is coded in green, and either the protein or peptide is coded in blue. The rescaled maps (Fig. 5) demonstrate that both HSA and SUB-6 showed preferential adsorption to the interface, which was highlighted in blue under all conditions. Comparison of the PS regions for the three concentrations revealed a much more "pink" color arising from the maps of HSA in comparison to maps of SUB-6, indicative of protein preference in this region. At higher peptide concentrations, the

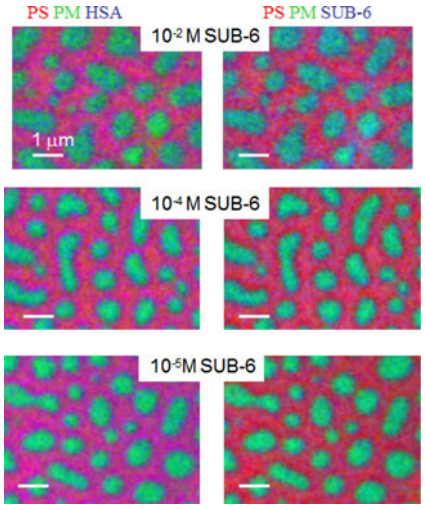

FIG. 5. Color-coded rescaled component maps for the SUB-6/HSA mix adsorbed to PS/PMMA at (top) SUB-6 concentration of 1×10^{-2} mg/ml; (middle) SUB-6 concentration of 1×10^{-4} mg/ml; (bottom) SUB-6 concentration of 1×10^{-5} mg/ml. Concentration of HSA was unchanged at 0.05 mg/ml.

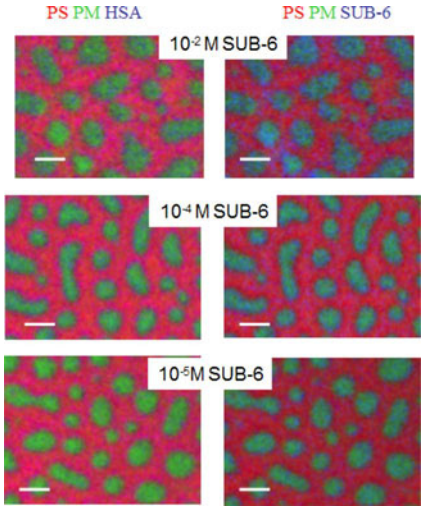

FIG. 6. Color-coded nonrescaled (absolute) component maps for the SUB-6/HSA mix adsorbed to PS/PMMA at (top) SUB-6 concentration of 1×10^{-2} mg/ml; (middle) SUB-6 concentration of 1×10^{-4} mg/ml; (bottom) SUB-6 concentration of 1×10^{-5} mg/ml. Concentration of HSA was unchanged at 0.05 mg/ml

TABLE III. Thickness of SUB-6 and HSA (nm/pixel) on the PS and PMMA domains and at the PS/PMMA interface for adsorption from a mixed SUB-6/HSA solution on a PS/PMMA blend at three SUB-6 concentrations. HSA concentration held constant at 0.05 mg/ml. Uncertainty is ±0.5 nm.

		Thickness (nm) Concentration of SUB-6 ([HSA]=0.05 mg/ml)		
Region	Composite (nm/pixel)	1×10^{-2}	1×10^{-4}	1×10^{-5}
PS	PS	7.5	7.7	8.5
	PMMA	0.0	0.0	0.0
	HSA	1.6	1.5	1.6
	SUB-6	0.8	0.9	0.0
PMMA	PS	1.9	1.3	1.9
	PMMA	3.4	4.3	5.2
	HSA	1.6	1.7	1.5
	SUB-6	3.3	2.7	1.5
Interface	PS	3.0	3.9	4.8
	PMMA	1.3	1.8	1.9
	HSA	2.1	2.4	2.6
	SUB-6	3.5	1.9	0.8

domains of PMMA were strongly colored in blue; however, as the concentration decreased, the color of the PS/PMMA/HSA and PS/PMMA/SUB-6 maps were comparable, illustrating similar site preference for both protein and peptide.

The absolute maps (Fig. 6) also revealed strong adsorption by both HSA and SUB-6 at the interface. Most striking are the very blue domains found for SUB-6 at higher concentration. As the concentration decreased, the color on the domains became lighter, yet preference for PMMA was still seen. The PS region was contrasted sharply between the pink color arising from the protein and the very "red" color from the peptide. These images clearly illustrate the site preference of SUB-6 and HSA for the PMMA and PS regions, respectively.

Adsorption in the HSA/SUB-6 system is likely to have been complicated by possible ionic complex formation between the negatively charged HSA and positively charged SUB-6. These interactions can lead to protein unfolding and conformational change.[25] In fact, dynamic light scattering of a HSA/amphiphilic drug complex revealed the presence of micelles in solution.[25] However, it seems unlikely that the hydrophilic SUB-6 peptide will form micelles with HSA due to the evenly spaced positive charge along the peptide chain. Also, at peptide concentrations below 1×10^{-4} mg/ml SUB-6, the number of HSA molecules greatly exceeded the number of SUB-6 molecules (in solution the concentration of HSA was $7.6\times10^{-7}M$ while SUB-6 was only $5.5\times10^{-9}M$). Nonetheless, SUB-6 remained highly surface active, as shown in Sec. IV B. Thus, for the mixture of coadsorbing HSA/SUB-6 two competing processes can occur: (1) individual adsorption of the protein or peptide molecules and (2) adsorption of a protein-peptide complex formed in solution by electrostatic attraction.

This complexity was most evident in the PMMA region where the two processes likely occurred simultaneously

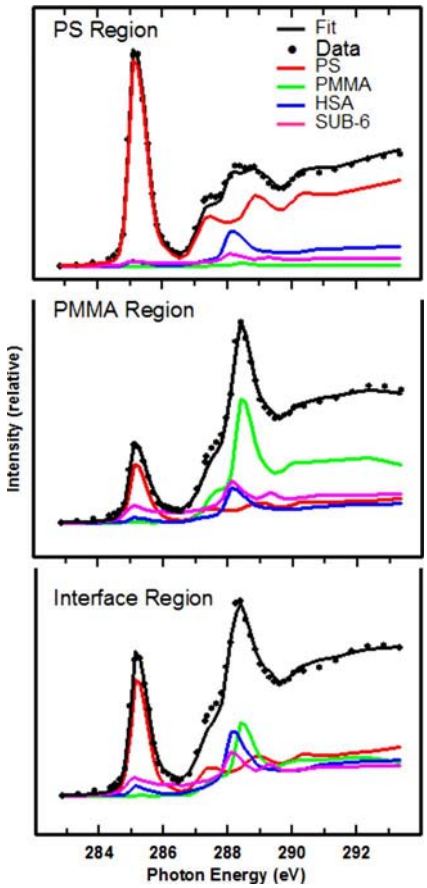

FIG. 7. Curve fits of the C 1*s* spectra extracted from the PS, PMMA, and interface regions for adsorption from the mixture of 0.05 mg/ml HSA with 0.01 mg/ml SUB-6 at *p*H (PS in red, PMMA in green, HSA in blue, and SUB-6 in pink)

(Table III, Fig. 7). In this region, substantial amounts of both HSA and SUB-6 were detected in a competitive (individual) adsorption-type process; however, the thickness of HSA adsorbed from the biomixture was markedly lower than when the polymer surface was exposed to HSA alone. SUB-6 was highly surface active in the PMMA region which may account for lower surface area availability, leading to decreased HSA adsorption. In contrast, adsorption of SUB-6 from the mixture was sharply elevated compared to adsorption of SUB-6 by itself. Thus, the quantitative analyses suggest that an electrostatic complex must be present, and that the complex had a high affinity for the PS/PMMA surface to account for the higher thickness of adsorbed peptide. In this case, based on charge considerations, a $[\mathrm{HSA(SUB-6)_3}]$ complex is likely to have formed, leading to a greater thickness of peptide. Studies are underway to characterize this postulated complex via gel electrophoresis (SDS-PAGE), mass spectrometry, and high field nmr.

The interpretation of the adsorption on the PS region was simpler. Since SUB-6 adsorption to PS was low, the dominant mechanism is likely adsorption by the protein/peptide complex. This explanation was supported by the lower adsorption thickness of HSA from the biomixture compared to adsorption of HSA itself and also slightly higher adsorption values for SUB-6 from the mixture compared to the pure peptide solution. Since a charge neutralizing complex would be formed, the negative charge of HSA was decreased. Hence, the adsorbed thickness of approximately 1.6(5) nm was much closer to the values recorded for the protein at the isoelectric point [at *p*H 4, HSA thickness ~1.4(5) nm].[12] In addition, since the complex formation likely led to conformational change in the protein, the new HSA/SUB-6 species was probably more hydrophilic, also leading to less protein adsorption on the hydrophobic PS region.

At the interdomain interface, the dominant mechanism is considered to be individual peptide/protein competitive adsorption which arises from favorable thermodynamic and kinetic considerations. Both HSA and SUB-6 selectively adsorb to the interdomain region; however, this region is small and easily saturated.[10] Quantitative analyses indicate that the electrostatic complex was a minor adsorbed component in this region since the thickness of SUB-6 adsorbed from the biomixture was much closer to the value for adsorption from the pure peptide solution than was the case at the PMMA region. As the concentration of peptide was decreased, the thickness of protein systematically increased until the thickness was comparable to the pure protein solution adsorption values.[13]

Although the adsorption of the biocomponents in this system is proposed to be primarily driven by hydrophobic interactions, since electrostatic double layers are weak surrounding the uncharged substrate, there is some evidence for small contributions to the preferential adsorption from charged interactions of the peptide For example, the positively charged SUB-6 showed a much higher preference for the polar carbonyl groups of PMMA. In contrast, the adsorption behavior of the "soft" HSA is known to be driven by gains in conformational entropy.[26]

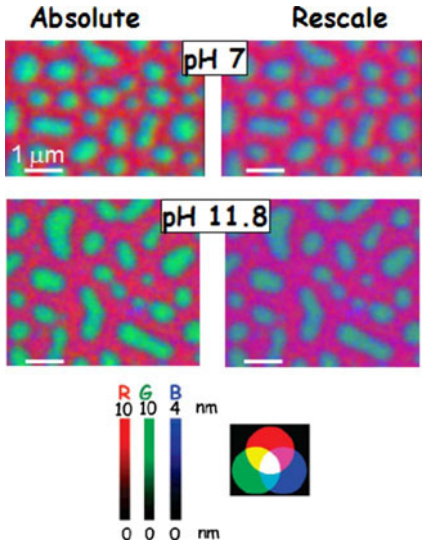

FIG. 8. Color-coded component maps (left, rescaled; right absolute) for adsorption on a PS/PMMA blend surface from a solution of pure SUB-6 (1×10^{-2} mg/ml) at (top) neutral *p*H (7.2) and (bottom) alkaline *p*H (11.8).

Due to the combination of electrostatic attraction and the unique aspects of the NEXAFS spectrum of SUB-6, X-PEEM was capable of detecting the peptide at concentrations as low as $5\times10^{-9}M$ (5 nM or 0.1 ng/ml). This extremely low detection limit exceeds the current detection limits of several surface sensitive techniques such as MALDI-MS (0.6 ng/ml),[27] surface plasmon resonance (50 ng/ml),[28] and resonance light scattering (15 ng/ml).[29] It is worth noting that X-PEEM provides this very low averaged detection limit while at the same time providing high (50 nm) lateral spatial resolution in the surface distributions. NEXAFS is also capable of detecting the four chemical components of this system (PS, PMMA, HSA, and SUB-6) simultaneously in a quantitative fashion as is clearly demonstrated to the least-squares fits to the extracted spectra (Fig. 7). Careful analyses of these spectral fits reveal that removal of either the peptide or the protein component leads to a visible misfit and substantial increase in the residual spectrum.

D. Effect of *p*H

1. Changes in SUB-6 adsorption

To evaluate the electrostatic effect of SUB-6 adsorption, the *p*H was raised to neutralize the positive charge on the peptide. The acid dissociation constant for the guanidine group of arginine ranges from $\log K_1 \sim 10.78$ to 15.0, depending on the ionic strength.[30] At extremely alkaline *p*H, the PS/PMMA film deteriorates; thus, all measurements were carried out at *p*H 11.8.

Figure 8 compares the color-coded composite maps derived from 1×10^{-2} mg/ml SUB-6 adsorbed onto the PS/PMMA blend surface at neutral and alkaline *p*H. The res-

TABLE IV. Thickness of SUB-6 and SUB-6/HSA mix (nm/pixel) on the PS and PMMA domains and at the PS/PMMA interface at alkaline *p*H. Uncertainty is ±0.5 nm.

Region	Composite (nm/pixel)	Thickness (nm) SUB-6 (*p*H 11.8) 0.01 mg/ml	Thickness (nm) SUB-6/HSA mix (*p*H 11.8) 0.01/0.05 mg/ml
PS	PS	7.6	7.0
	PMMA	0.2	0.2
	HSA		1.7
	SUB-6	2.2	1.1
PMMA	PS	1.7	1.7
	PMMA	5.7	5.0
	HSA		0.6
	SUB-6	2.6	2.7
Interface	PS	4.1	3.6
	PMMA	2.4	2.1
	HSA		1.6
	SUB-6	3.5	2.9

caled images demonstrate that the interface was still the site of preferential protein adsorption at alkaline *p*H; however, the absolute images clearly reveal that at basic *p*H the amount of SUB-6 on the PS regions had increased substantially, since the PS regions shows a much more pink color than at neutral *p*H. In contrast, the amounts of SUB-6 on the PMMA domains and at the interface remained rather similar.

The quantitative spectral analyses support the results from the mapping (Table IV). At alkaline *p*H, the thickness of SUB-6 on the PS region had substantially increased to 2.2(5) nm, in contrast to the 0.8(5) nm thickness at neutral *p*H. Interestingly, the adsorbed thickness on both the PMMA and interface regions remained the same within the limits of uncertainty. As expected, the preferential adsorption at the interdomain region prevailed regardless of charge. A slight decrease in adsorbed PMMA thickness was expected; however, at *p*H 11.8 not all of the protons from the guanidine groups would be removed and thus it is proposed that a fraction of the positively charged peptide adsorbed at the PMMA region.

2. Redistribution of SUB-6 and HSA

The coadsorption of SUB-6 (1×10^{-2} mg/ml) and HSA (0.05 mg/ml) was also examined at alkaline *p*H (*p*H=11.8). It is assumed that at this *p*H most of the protons from the guanidine group of arginine are removed, suppressing the formation of the electrostatic complex. Thus, at high *p*H, the mode of competitive adsorption was based mainly on the individual properties of the HSA protein and SUB-6 peptide. The color-coded composite maps are shown with both rescaled and absolute presentations in Fig. 9. The rescaled maps reveal the preference of both SUB-6 and HSA for the interface. However, the absolute maps show that there was a decrease in protein/peptide adsorption on the PMMA domains, hence there was a redistribution of the biocomponents.

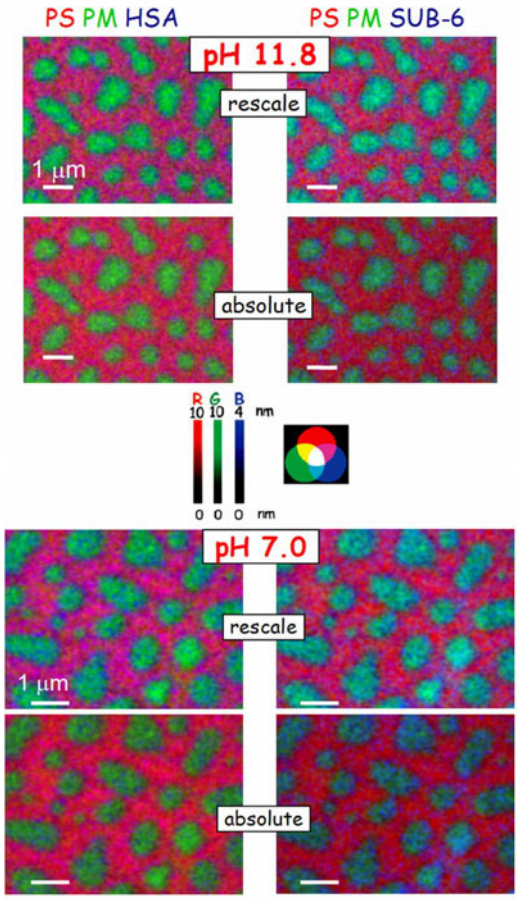

FIG. 9. Color-coded component maps (upper, rescaled; lower, absolute) for adsorption on a PS/PMMA blend surface from solutions of a mixture of SUB-6 (1×10^{-2} mg/ml) and HSA (0.05 mg/ml) at (top) neutral *p*H (7.2) and (bottom) alkaline *p*H (11.8).

The results from the spectral fits showed an increase in the thickness of SUB-6 adsorbed at the PS region, which paralleled the increased adsorption of SUB-6 on the PS region for the pure peptide alkaline solution. The corresponding HSA thickness on PS was similar to the thickness adsorbed at neutral *p*H (Table IV). More importantly, this thickness value was within the uncertainty of measurements of the adsorption of pure HSA at *p*H 10.0 to PS/PMMA at the PS region.[11]

At the PMMA and interdomain regions, the charge neutralizing effect resulting in the elimination of the electrostatic complex was evident. At the PMMA domains the thickness of adsorbed peptide was similar to the amount of peptide adsorbed from the pure SUB-6 solution. Nonetheless, HSA adsorption was substantially lower at alkaline *p*H than at neutral *p*H which suggested that the PMMA domains were primarily covered by the peptide, leaving a smaller amount of surface area for HSA adsorption.

As previously discussed, the interdomain region is easily saturated; therefore, the dominant adsorption mechanism was individual competitive adsorption. As illustrated from the quantitative analyses, the adsorption of both HSA and SUB-6 decreased slightly as the *p*H was elevated; however, since

the HSA adsorbed thickness did not drastically decrease (removal of protein-peptide attraction), the previous conclusion that complex formation is only a minor component was supported.

V. SUMMARY

We have shown that X-PEEM is capable of differentiating and mapping HSA protein and SUB-6 peptide adsorbed on a phase-segregated PS/PMMA polymer blend surface from a mixture at very low concentrations, as low as 5×10^{-9} mol/l or 0.1 ng/ml in the SUB-6 peptide. The preferential adsorption of the peptide was elucidated both in pure SUB-6 solutions and in a mixture of protein and peptide at neutral and alkaline *p*H. The results were explained in terms of formation of an electrostatic complex between the positively charged peptide and the negatively charged protein, which has an adsorption behavior which depends on the polarity of the different domains of the PS/PMMA substrate. As the *p*H was raised to neutralize the charge on the peptide, complex formation was suppressed and a more competitive-type adsorption process was observed.

ACKNOWLEDGMENTS

This research was supported by the Natural Science and Engineering Research Council (NSERC, Canada), AFMNet and the Canada Research Chair programs. X-ray microscopy was carried out using PEEM2 at the ALS. The ALS is supported by the U.S. Department of Energy under Contract No. DE-AC03-76SF00098.

[1]H. Ade, *Experimental Methods in the Physical Sciences* (Academic, New York, 1998), Chap. 32.
[2]H. Ade and S. G. Urquhart, *Chemical Applications of Synchrotron Radiation* (World Scientific, Singapore, 2002), pp. 285–355.
[3]H. Ade and A. P. Hitchcock, Polymer **49**, 643 (2008).
[4]J. R. Lawrence, G. D. Swerhone, G. G. Leppard, T. Araki, X. Zhang, M. M. West, and A. P. Hitchcock, Appl. Environ. Microbiol. **69**, 5543 (2003).
[5]K. Kaznacheyev, A. Osanna, C. Jacobsen, O. Plashkevych, O. Vahtras, H. Ågren, V. Carravetta, and A. P. Hitchcock, J. Phys. Chem. A **106**, 3153 (2002).
[6]Y. Zubavichus, A. Shaporenko, M. Grunze, and M. Zharnikov, J. Phys. Chem. A **109**, 6998 (2005).
[7]J. Stewart-Ornstein, A. P. Hitchcock, D. Hernandez-Cruz, P. Henklein, J. Overhage, K. Hilpert, J. D. Hale, and R. E. W. Hancock, J. Phys. Chem. B **111**, 7691 (2007).
[8]Y. Zubavichus, A. Shaporenko, M. Grunze, and M. Zharnikov, J. Phys. Chem. C (to be published).
[9]K. Hilpert, R. Volkmer-Engert, T. Walter, and R. E. W. Hancock, Nat. Biotechnol. **23**, 1008 (2005).
[10]C. Morin, A. P. Hitchcock, R. M. Cornelius, J. L. Brash, S. G. Urquhart, A. Scholl, and A. Doran, J. Electron Spectrosc. Relat. Phenom. **137–140**, 785 (2004).
[11]L. Li, A. P. Hitchcock, N. Robar, R. Cornelius, J. L. Brash, A. Scholl, and A. Doran, J. Phys. Chem. B **110**, 16763 (2006).
[12]L. Li, A. P. Hitchcock, R. Cornelius, J. L. Brash, A. Scholl, and A. Doran, J. Phys. Chem. B **112**, 2150 (2008).
[13]L. Li, J. L. Brash, R. Cornelius, A. Scholl, A. Doran, and A. P. Hitchcock (unpublished).
[14]C. Morin *et al.*, J. Electron Spectrosc. Relat. Phenom. **121**, 203 (2001).
[15]D. Romeo, B. Skerlavaj, M. Bolognesi, and R. Gennaro, J. Biol. Chem. **263**, 9573 (1988).
[16]S. Anders *et al.*, Rev. Sci. Instrum. **70**, 3973 (1999).
[17]J. Wang, L. Li, C. Morin, A. P. Hitchcock, A. Doran, and A. A. Scholl, J. Electron Spectrosc. Relat. Phenom. (to be published).
[18]C. J. Jacobsen, S. Wirick, G. Flynn, and C. Zimba, J. Microsc. **197**, 173 (2000).
[19]T. Warwick *et al.*, J. Synchrotron Radiat. **9**, 254 (2002).
[20]A. L. D. Kilcoyne *et al.*, J. Synchrotron Radiat. **10**, 125 (2003).
[21]B. L. Henke, E. M. Gullikson, and J. C. Davis, At. Data Nucl. Data Tables **54**, 181 (1993).
[22]aXis2000 is free for noncommercial use. It is written in Interactive Data Language (IDL) and available from http://unicorn.mcmaster.ca/aXis2000.html
[23]G. Strang, *Linear Algebra and its Applications* (Harcourt Brace Jovanovitch, San Diego, 1988).
[24]I. N. Koprinarov, A. P. Hitchcock, C. T. McCrory, and R. F. Childs, J. Phys. Chem. B **106**, 5358 (2002).
[25]D. Leis, S. Barbosa, D. Attwood, P. Toboada, and V. Mosquera, J. Phys. Chem. B **106**, 9143 (2002).
[26]K. Nakanishi, T. Sakiyama, and K. Imamura, J. Biosci. Bioeng. **91**, 233 (2001).
[27]Y. Xu, J. Throck Watson, and M. L. Bruening, Anal. Chem. **75**, 185 (2003).
[28]M. Suzuki, F. Ozawa, W. Sugimoto, and S. Aso, Anal. Bioanal. Chem. **372**, 301 (2002).
[29]L. Wang, H. Chen, L. Li, T. Xia, L. Dong, and L. Wang, Spectrochim. Acta, Part A **60**, 747 (2004).
[30]O. Yamauchi and A. Odani, Pure Appl. Chem. **68**, 469 (1996).